Interactions between hydrogen impurities and vacancies in Mg and Al: A comparative analysis based on density functional theory

Lars Ismer,[1,2] Min Sik Park,[1,3] Anderson Janotti,[1] and Chris G. Van de Walle[1]
[1]*Materials Department, University of California, Santa Barbara, California 93106-5050, USA*
[2]*Abteilung Computergestütztes Materialdesign, Max-Planck-Institut für Eisenforschung GmbH, Max-Planck-Strasse 1, 40237 Düsseldorf, Germany*
[3]*Department of Physics, Missouri University of Science and Technology, Rolla, Missouri 65409, USA*
(Received 24 July 2009; revised manuscript received 16 October 2009; published 17 November 2009)

Using first-principles methods we have studied the interactions between hydrogen impurities and vacancies in hcp Mg and fcc Al. We find that single vacancies can, in principle, host up to 9 H atoms in Mg and 10 in Al, not 12 as recently reported in the case of Al. The difference between our results and the results in previous work is attributed to a more appropriate definition of the trapping energy of hydrogen impurities in vacancies. The concentration of hydrogen-vacancy complexes depends on the amount of hydrogen dissolved in the metal, which in turn is dictated by the hydrogen chemical potential μ_H. We evaluated the concentration of all relevant hydrogen-vacancy complexes as a function of μ_H, corresponding to different H loading conditions—ranging from low pressures to high pressures of H_2 gas, up to hydrogen plasma conditions. Our analysis reveals fundamental differences in the characteristics of the hydrogen-vacancy interaction between Mg and Al. In the case of Al, up to 15% of H atoms are trapped in single vacancies in the form of H-vacancy complexes even for very low values of μ_H. The trapping effect slows down the diffusion of H atoms in Al by more than an order of magnitude. While interactions between vacancies and *single* hydrogen atoms are therefore clearly important, interactions with *multiple* H atoms and related mechanisms (such as hydrogen-induced superabundant vacancy formation) are predicted to occur in Al only at very high values of μ_H. In the case of Mg, the effects of H trapping in single vacancies are negligible for low values of μ_H due to the relatively low formation energy of isolated interstitial H. However, vacancies containing multiple H atoms and related mechanisms such as hydrogen-induced superabundant vacancy formation are predicted to occur in Mg at much lower values of μ_H than in Al. We estimate that, at room temperature, the critical pressure of an H_2 gas to induce hydrogen-enhanced (superabundant) vacancy formation is ~ 1 GPa in Mg and ~ 10 GPa in Al.

DOI: 10.1103/PhysRevB.80.184110 PACS number(s): 71.15.Nc, 71.55.Ak, 61.72.J−, 66.30.J−

I. INTRODUCTION

Al-based and Mg-based hydrides have great potential as hydrogen storage materials due to their light weight and high hydrogen capacities.[1] Ideally, these materials would reversibly release H_2 upon heating, with Al and Mg being the byproducts or reactants in the hydrogen desorption or uptake processes. In order to be able to engineer the hydrogen desorption and uptake at suitable temperatures and with adequate kinetics, it is essential to understand the related atomistic mechanisms. With that goal in mind, we have studied the effects of hydrogen on the structural properties of Al and Mg. The presence of vacancies and their interactions with hydrogen impurities in the bulk of the metal is expected to play an important role in the kinetics of the desorption/uptake processes.

Aluminum has been the subject of various experimental and theoretical investigations regarding the effects of hydrogen impurities.[2–9] Experimental studies suggested that hydrogen atoms are trapped at vacancies, leading to a significant reduction in the H diffusion rates in Al crystals.[6] This trapping hypothesis has been corroborated by first-principles calculations which led to models for describing the observed diffusion rates.[7,9] Lu and Kaxiras[8] suggested that, in principle, up to 12 H atoms can be accommodated in a single vacancy in Al and that the trapping of multiple H atoms in a single vacancy can overcompensate the energy cost to form the defect. Moreover, trapping of multiple H atoms in a single vacancy in Al could be related to the observed hydrogen-induced superabundant vacancy formation and vacancy clustering. These effects may play an important role in hydrogen embrittlement processes as well as in hydride formation.[8] More recently, Gunaydin *et al.*[9] reported that trapping of multiple H atoms in a single vacancy in Al is possible only for extreme H loading conditions, i.e., for H concentrations many orders of magnitude above the solubility limit given by the equilibrium with H_2 gas at ambient conditions (10^{-9} at 300 K and 1 atm). Instead, at the H loading conditions used in most diffusion experiments, empty vacancies would coexist with vacancies filled by one or at most two H atoms.

These seemingly conflicting results, from Lu and Kaxiras[8] on the one hand and from Gunaydin *et al.*[9] on the other hand, indicate that the understanding of the interactions between hydrogen impurities and vacancies in Al is still far from complete. For instance, it is unclear for which values of the hydrogen chemical potential μ_H the H-enhanced (superabundant) vacancy formation will occur; or what is the concentration ratio between H in hydrogen-vacancy complexes and H at the interstitial sites. At an even more basic level, the energy required or released when adding an H atom to a vacancy that already contains n H atoms has not been reported. In order to address these issues, one needs to know the absolute formation energies of vacancies, interstitial hy-

drogen, and hydrogen-vacancy complexes, and their dependence on the hydrogen chemical potential μ_H.

The interactions of hydrogen impurities with vacancies in Mg has been much less explored.[5,10] Mg is also a lightweight metal and has one less valence electron than Al. Mg and Al crystallize in different structures (hcp for Mg and fcc for Al) with different equilibrium volumes per atom. Recent experimental studies revealed that the vacancy concentration in Mg is strongly affected by the presence of hydrogen impurities, i.e., depending on whether the material has been prepared in a hydrogen-rich or in a hydrogen-poor environment.[11] Motivated by the conflicting results in Al and the lack of information in the case of Mg, we have performed a detailed comparison between Al and Mg regarding the interaction of hydrogen impurities with single vacancies. Based on state-of-the-art first-principles calculations we have evaluated the concentrations of interstitial hydrogen and hydrogen-vacancy complexes as a function of μ_H, corresponding to different H loading conditions—ranging from low pressures to high pressures of H_2 gas, up to hydrogen plasma conditions. This analysis allows us to uncover fundamental differences in the characteristics of the hydrogen-vacancy interactions between Al and Mg.

II. METHODS

In order to evaluate the concentration of the interstitial hydrogen and hydrogen-vacancy complexes we calculated formation energies as described in Ref. 12. Assuming that the defects are in the dilute limit, their concentration at a given temperature is determined by their formation energy[12]

$$c = N_{\text{sites}} N_{\text{config}} \exp\left(-\frac{E_f}{k_B T}\right), \tag{1}$$

where N_{sites} is the number of lattice sites on which the defect can be incorporated and N_{config} is the number of equivalent configurations per site. We will use the convention to express all the concentrations as "per lattice site." The formation energy E^f of a defect X is defined as[12]

$$E^f(X) = E_{\text{tot}}(X) - E_{\text{tot}}(\text{bulk}) - \Sigma_i n_i \mu_i, \tag{2}$$

where $E_{\text{tot}}(X)$ is the total energy of the supercell containing the defect and $E_{\text{tot}}(\text{bulk})$ is the total energy of the perfect bulk in the same supercell. The quantity μ_i is the chemical potential of species i and n_i is the number of atoms of species i added to $(n_i > 0)$ or removed from $(n_i < 0)$ the supercell to form the defect. More details about the chemical potentials, in particular, for hydrogen, will be given below.

The total energies required in Eq. (2) were determined by performing first-principles calculations based on density functional theory (DFT) in the generalized gradient approximation[13] and the projector-augmented wave (PAW) method.[14] Hence, the electronic structure of the host materials is explicitly taken into account, with the wave functions expanded in a plane-wave basis set using an energy cutoff of 270 eV. The defects were simulated using the supercell approach, with 32-atom supercells for fcc Al and 48-atom supercells for hcp Mg; integrations over the Brillouin zone were performed by using a mesh of $8\times8\times8$ or $6\times6\times6$ k points, respectively. Equilibrium geometries were determined by fully relaxing the atoms in the supercell. All calculations were performed using the Vienna *ab initio* simulation package.[15]

The migration paths were determined for a path between two adjacent lattice sites that correspond to equivalent configurations for the ground state of the defect. The energies along the path were calculated by taking up to nine points along a line connecting the initial and final positions, and allowing the migrating species (as well as surrounding atoms) to fully relax in a plane perpendicular to the migration direction. The saddle-point configuration is determined by finding the maximum in the energy along this path, and the migration barrier is the energy difference between the ground-state and the saddle-point configurations.

In order to obtain accurate absolute values for the free energy of formation of H impurities in the host metal, it is necessary to include the contributions from zero-point energy (ZPE). In the present work, when calculating concentrations, we use the results for ZPEs obtained in previous first-principles studies.[7] The ZPE contribution to the formation energy, which is the difference between half of the zero-point vibration energy of the H_2 molecule and the zero-point vibration energy of the H atom in the solid, amounts to $\Delta E^{f,\text{ZPE}} = 0.08$ eV in the case of H in Al. Here we use this value for Al and also use it as an approximation in the case of interstitial H in Mg. Furthermore, we assume that the ZPE contribution to the formation energy for H on vacancy sites can be approximated by the ZPE of H on interstitial sites.

III. RESULTS

A. Formation of interstitial hydrogen

First we discuss the results for the formation energy of an H atom at the interstitial site in fcc Al and hcp Mg. The lowest-energy configuration for interstitial H in the fcc-Al and hcp-Mg lattices was determined by placing an H atom at all possible interstitial positions. We find that interstitial H in fcc Al and hcp Mg is locally stable at the two high-symmetry interstitial sites: the tetrahedral (T_d) site and the octahedral (O_h) site, schematically shown in Fig. 1. In both Al and Mg, the tetrahedral site is lower in energy than the octahedral site. The calculated formation energies with respect to the energy of an H atom in the H_2 molecule (at $T=0$ K and without including zero-point vibration energy) are listed in Table I.

As a remarkable difference between fcc Al and hcp Mg, we find that the formation energy for interstitial hydrogen, $E^f(T_d)$ in Table I, is significantly lower in Mg than in Al. This implies that, for a given hydrogen chemical potential, a much higher concentration of interstitial hydrogen can be dissolved in Mg than in Al. For example, using Eq. (1), the interstitial H concentration in Mg is more than nine orders of magnitude higher than in Al at room temperature.

The difference in the formation energy of interstitial H in fcc Al and hcp Mg can be understood by decomposing it in three parts: first, the contribution from different lattice types (fcc versus hcp); second, the difference between the equilibrium volumes (Mg has a larger equilibrium volume than Al);

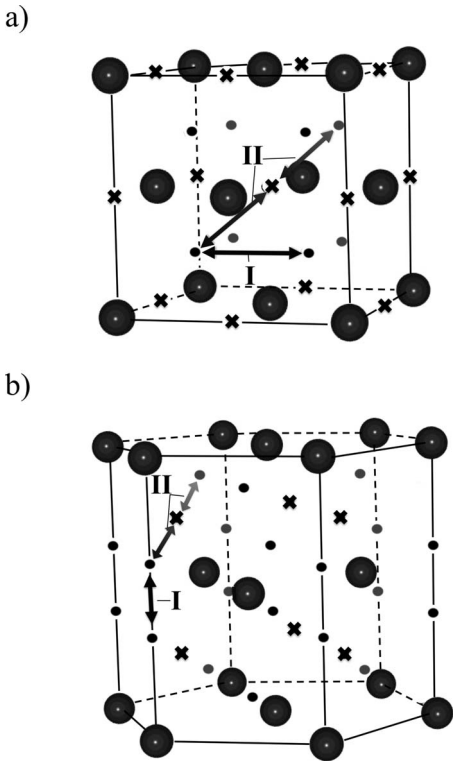

FIG. 1. Interstitial lattice sites and lowest-energy diffusion paths for H in (a) fcc Al and (b) hcp Mg. The balls denote the lattice atoms, whereas the dots and crosses denote the tetrahedral and octahedral interstitial lattice sites, respectively. The diffusion paths for interstitial H are indicated and the corresponding energy barriers are listed in Table I.

and third, the difference due to electronic structure (Mg has one less valence electron than Al). The difference in formation energies can then be written as

$$\Delta E^f(T_d) = E^f(T_d,\mathrm{Al}) - E^f(T_d,\mathrm{Mg}) \tag{3}$$

$$= \Delta E^f_{\mathrm{fcc}\leftarrow\mathrm{hcp}}(T_d) + \Delta E^f_{vol}(T_d) + \Delta E^f_{el}(T_d). \tag{4}$$

The three contributions have been calculated as follows. $\Delta E^f_{\mathrm{fcc}\leftarrow\mathrm{hcp}}(T_d)$ is the difference in formation energies of H (at the tetrahedral interstitial site) in fcc Mg and hcp Mg, both at the lattice constant corresponding to the equilibrium lattice volume of hcp Mg. $\Delta E^f_{vol}(T_d)$ is the difference between formation energies of interstitial H in fcc Al at the Al equilibrium lattice constant and fcc Al at the lattice constant corresponding to the equilibrium lattice volume of hcp Mg. $\Delta E^f_{el}(T_d)$ is the difference in formation energies between fcc Al and fcc Mg at the lattice constant corresponding to the equilibrium lattice volume of hcp Mg. This decomposition is arbitrary to some degree. For example, one could take the volume term for Mg (instead of Al) or calculate the electronic term at the fcc-Al equilibrium lattice volume (instead of the hcp-Mg equilibrium lattice volume). However, we found that the variations for the individual terms between the various possible decompositions are rather small (less than 0.1 eV).

TABLE I. Formation energies and diffusion energy barriers of interstitial hydrogen in fcc Al and hcp Mg. $E^f(T_d)$ and $E^f(\mathrm{O}_h)$ denote the formation energies [see Eq. (2)] at the tetrahedral and octahedral interstitial lattice sites, respectively. The formation energies are referenced to H_2 and bulk metal at $T=0$ K and do not include zero-point vibration energies. $E^b(\mathrm{I})$ and $E^b(\mathrm{II})$ denote the diffusion energy barriers associated with the diffusion paths I and II illustrated in Fig. 1. Results from previous theoretical and experimental studies are also listed for comparison. All energies in eV.

Property	Observable	Al	Mg
H solution	$E^f(\mathrm{O}_h)$	0.77	0.26
	$E^f(T_d)$	0.68	0.12
	$E^f_{calc}(T_d)$	0.69[a]	
	E^f_{exp}	0.60–0.71[b]	
H diffusion	$E^b(\mathrm{I})$	0.33	0.08
	$E^b(\mathrm{II})$	0.17	0.22
	$E^b_{calc}(\mathrm{II})$	0.18[a]	0.19[d]
	E^b_{exp}	0.16[c]	0.24[e]

[a]Reference 7 (DFT GGA).
[b]References 16–20.
[c]Reference 6.
[d]Reference 21 (DFT GGA).
[e]Reference 22.

From the values listed in Table II we note that the contribution due to volume dominates and that the effect due to different lattice structures is smallest: $|\Delta E^f_{vol}| > |\Delta E^f_{el}| > |\Delta E^f_{\mathrm{fcc}\leftarrow\mathrm{hcp}}|$. Hence, the lower formation energy for interstitial H in hcp Mg compared to fcc Al is largely due to the volume effect, i.e., the fact that Mg provides a larger interstitial embedding volume for the hydrogen atoms. The differences in the electronic structure and those in the lattice types (hcp versus fcc) between Mg and Al play a much smaller role.

B. Migration of interstitial hydrogen

We also investigated the migration of an interstitial H atom in the fcc-Al and hcp-Mg lattices. The lowest-energy migration paths in the fcc-Al lattice are schematically shown in Fig. 1(a). In principle, the symmetry of the fcc lattice allows for two different migration paths. In the first, labeled as path I in Fig. 1(a), interstitial H migrates to an adjacent (nearest-neighbor) tetrahedral interstitial site passing through a "bond-center" site (point in the middle of two nearest-neighbor Al sites). In path II the interstitial H migrates to a

TABLE II. Decomposition of the difference between the formation energy of interstitial hydrogen in Mg and Al [see Eq. (4)]. All energies in eV.

$\Delta E^f(T_d)$	0.56
$\Delta E^f_{\mathrm{fcc}\leftarrow\mathrm{hcp}}(T_d)$	–0.09
$\Delta E^f_{vol}(T_d)$	0.45
$\Delta E^f_{el}(T_d)$	0.20

TABLE III. Formation energies and diffusion barriers of vacancies in fcc Al and hcp Mg. E^f and E^b denote the formation energies and energy barriers [see Eq. (2)] at $T=0$ K, not including zero-point vibration energies. Results from previous theoretical and experimental studies are also included. All energies in eV.

Property	Observable	Al	Mg
V formation	E^f	0.62	0.74
	E^f_{calc}	0.54[a], 0.78[b]	0.80[b]
	$E^f_{\exp}$	0.66[c]	0.56–0.90[d]
V diffusion	E^b	0.52	0.41
	E^b_{calc}	0.66[b]	0.43[b]
	$E^b_{\exp}$		0.51–0.62[d]

[a]Reference 7 (DFT GGA).
[b]Reference 24 (DFT LDA).
[c]Reference 23.
[d]Reference 11 and references therein.

second-nearest-neighbor tetrahedral interstitial site, passing through an octahedral interstitial site. We find that the energy barrier for path II is significantly lower than that for path I, in agreement with the results reported in Ref. 7.

The lowest-energy migration paths for interstitial H in hcp Mg are schematically shown in Fig. 1(b). In path I an interstitial H atom moves to a nearest-neighbor tetrahedral interstitial site. However, in the hcp lattice the tetrahedral interstitial sites are arranged in pairs. Long-range migration of an interstitial H in an hcp lattice requires the H atom to jump between sites that belong to different pairs of tetrahedral interstitial sites. That is, long-range migration necessarily involves migration through path II, which passes through an intermediate octahedral interstitial site [Fig. 1(b)]. The barrier associated with path II is therefore the relevant barrier for migration of an interstitial H in hcp Mg.

The calculated migration energy barriers E^b for interstitial H in fcc Al and hcp Mg, for both paths I and II, are listed in Table I. Note that the energy barrier for path I in hcp Mg is very low but as noted above this path does not allow for long-range migration but only for hopping within a pair of neighboring tetrahedral sites.

The results presented in Table I for the formation energy and migration energy barriers of interstitial H in Al and Mg are in good agreement with available experimental results[6,16–20,22] as well as with previous theoretical studies, where available.[7,21]

C. Vacancy formation and migration

For completeness, we also investigated the stability and migration of vacancies in fcc Al and hcp Mg; the results are listed in Table III. We find that the formation energy of single vacancies is slightly higher in hcp Mg than in fcc Al and that the vacancy migration energy barrier is slightly lower in Mg than in Al. Note that these differences are relatively small. It is interesting to note that the sum of formation and migration energy, which is the activation energy of vacancy-mediated self-diffusion, is approximately equal in Mg and Al. Hence we expect the rates of self-diffusion via vacancy mechanisms to be the same in the two metals.

The results presented in Table III for the formation energy and migration energy barriers of vacancies in Al and Mg are in good agreement with available experimental results.[11,23] Our results also agree with previous theoretical studies;[7,24] the small differences are within the expected error bar of the DFT approach and may be attributed to the use of different exchange-correlation functionals [local-density approximation (LDA) is used in Ref. 24 instead of generalized gradient approximation (GGA) used in the present work] or different pseudopotentials (ultrasoft pseudopotentials are used in Ref. 7 while PAW potentials are used in the present work).

D. Hydrogen-vacancy complexes

We start the discussion of hydrogen-vacancy interactions in Al and Mg with the most basic process, i.e., the trapping of one H atom in a single vacancy. This process can be described by a "trapping energy," which is related to the energy gained by the system when one interstitial H atom is added to a single vacancy. For the first hydrogen added to an initially "empty" vacancy, the trapping energy is given by

$$E^{\text{trap}}(1) = E^f(V+\text{H}) - [E^f(V) + E^f(T_d)], \quad (5)$$

where $E^f(V+\text{H})$ is the formation energy of a hydrogen-vacancy complex in the host (fcc-Al lattice or hcp-Mg lattice), $E^f(V)$ is the formation energy of an isolated vacancy, and $E^f(T_d)$ is the formation energy of an isolated interstitial hydrogen. In both fcc Al and hcp Mg we find that $E^{\text{trap}}(1) < 0$, hence trapping one H in an initially empty vacancy is an exothermic process. We note, however, that $|E^{\text{trap}}(1)|$ in Al is larger than in Mg. In both cases, the H atom does not occupy the vacant substitutional metal site but prefers to sit very close (with a displacement of only 0.1 Å) to a tetrahedral interstitial site next to the vacant Al or Mg lattice site, as schematically shown in Fig. 3 for the fcc lattice.

We have also investigated the possibility of a single vacancy trapping more than one H atom. In this case, we define the trapping energy [Eq. (6)] as the energy difference between a vacancy containing n H atoms and a vacancy with $n-1$ H atoms plus an isolated H interstitial,

$$E^{\text{trap}}(n) = E^f(V+n\text{H}) - \{E^f[V+(n-1)\text{H}] + E^f(T_d)\}, \quad (6)$$

where $E^f(V+n\text{H})$ is the formation energy of a vacancy containing n H atoms. A negative value of $E^{\text{trap}}(n)$ therefore indicates that taking an interstitial H atom and adding it to a vacancy that already contains $n-1$ atoms is energetically favorable, with $|E^{\text{trap}}|$ being the energy gained in that process.

We calculated the formation energies for a number of (fully relaxed) configurations as candidates for the $V+n$H complex. In order to sufficiently sample the configurational space, we started from several different possible initial configurations for the $V+n$H complex, based on the structure of the lowest-energy $V+(n-1)$H complex plus an additional H atom placed at different positions in the vacancy. Using this procedure we find, in the case of Al, that $E^{\text{trap}}(n)<0$ for $n \leq 8$, as shown in Fig. 2 and Table IV.

Examining the local structure of the $V+n$H complexes, we find that in the relaxed geometric configurations of the

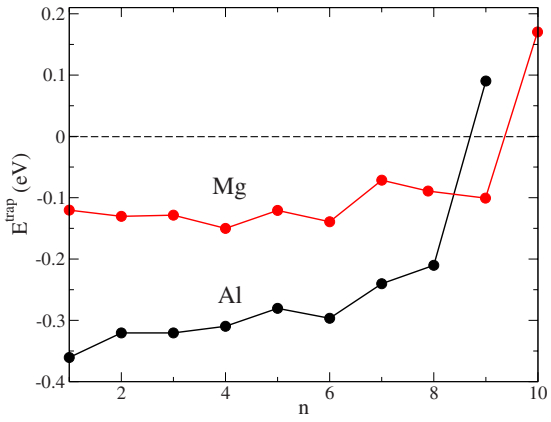

FIG. 2. (Color online) Calculated trapping energies of H atoms in vacancies in Al and Mg according to Eq. (6).

complexes with $n \leq 8$ all the H atoms occupy tetrahedral interstitial sites inside the vacancy, which we label "TV" sites. For the $V+n$H complexes with $E^{\text{trap}}[n]>0$ (i.e., $n<8$) all the TV tetrahedral sites are occupied and the additional H atoms occupy octahedral interstitial sites (labeled OV sites) inside the vacancy, which are less energetically favorable.

We have also investigated the possibility that hydrogen might be stored in molecular form (H_2) in the vacancy. Indeed we found *locally stable* configurations with one H_2 molecule located at the center of the Al vacancy, for all possible occupation numbers (i.e., $n=1-8$) of the TV sites. However, for $n<8$ these complexes are *thermodynamically* unstable since their formation energy is (for $n<6$) larger than that of the corresponding $V+(n+2)$H complex (with all H at TV sites) or (for $n=7$) larger than that of the $V+7$H complex plus two H atoms at interstitial lattice sites. Only for $n=8$, did we achieve a stable configuration, i.e., the formation energy of the $V+8\text{H}+\text{H}_2$ complex is lower than that of the $V+10$H complex (with 8 H at TV and 2 H at OV sites) *and* also lower than that of the $V+8$H complex plus 2 H atoms at interstitial lattice sites (i.e, $V+8\text{H}+2T_d$). This implies that in order for H_2 at the center of the vacancy to be stable, first all of the TV sites need to be occupied.

TABLE IV. Formation energies [Eq. (2) at $T=0$ K, not including zero-point vibration energies] and trapping energies [Eq. (6)] for all relevant hydrogen-vacancy complexes in Al and Mg. All energies in eV.

Host metal	Complex	E^f	E^{trap}
Al	V	0.62	
	$V+\text{H}$	0.94	−0.36
	$V+2\text{H}$	1.30	−0.32
	$V+3\text{H}$	1.66	−0.32
	$V+4\text{H}$	2.03	−0.31
	$V+5\text{H}$	2.43	−0.28
	$V+6\text{H}$	2.81	−0.30
	$V+7\text{H}$	3.25	−0.24
	$V+8\text{H}$	3.72	−0.21
	$V+7\text{H}+\text{H}_2$	4.49	0.09
	$V+8\text{H}+\text{H}_2$	4.99	
Mg	V	0.74	
	$V+\text{H}$	0.74	−0.12
	$V+2\text{H}$	0.73	−0.13
	$V+3\text{H}$	0.72	−0.13
	$V+4\text{H}$	0.69	−0.15
	$V+5\text{H}$	0.69	−0.12
	$V+6\text{H}$	0.67	−0.14
	$V+7\text{H}$	0.73	−0.06
	$V+8\text{H}$	0.76	−0.09
	$V+9\text{H}$	0.78	−0.10
	$V+10\text{H}$	1.07	0.17

The energy gain of the of the $V+8\text{H}+\text{H}_2$ complex with respect to $V+8\text{H}+2T_d$ amounts to 0.09 eV. Figure 2 does not include a value for the complex with 10 H because our definition of the trapping energy is not appropriate for this situation (with the complex with 9H being unstable). However, the formation energies of all stable complexes have been included in the thermodynamic analysis of concentrations that will be presented in Sec. III E.

The energetics of the trapping of hydrogen in single vacancies in Al can therefore be described as follows. Hydrogen is preferentially located in atomic form at TV sites. Due to a repulsive interaction of the H atoms inside the vacancy, which is reflected in a roughly linear increase in the trapping energy by ≈20 meV per H atom (see Fig. 2), trapping of additional H atoms becomes increasingly less energetically favorable as the number of H atoms in the vacancy increases. Once all eight TV sites are occupied ($n=8$), any additional hydrogen in *atomic* form is forced to occupy the less favorable OV sites. As a result, adding a ninth H atom becomes energetically unfavorable. However, the vacancy is able to host one additional H_2 *molecule*, resulting in a $V+8\text{H}+\text{H}_2$ complex.

Our results therefore show that, in principle, a single vacancy in Al can trap up to 10 H atoms. We note that this result differs from the conclusions reported by Lu and Kaxiras,[8] who suggested that up to 12 H atoms can be trapped in a single vacancy. We attribute the difference to the way in which the trapping energy is defined. Lu and Kaxiras used a different definition for the trapping energy,

$$E_{LK}^{\text{trap}}(n) = \frac{1}{n}[E^f(n\text{H}+V) - nE^f(T_d) - E^f(V)]. \qquad (7)$$

This quantity compares the energy of the $V+n$H complex to the energy of an isolated vacancy plus n H atoms at interstitial sites and expresses the result per H atom. We feel this quantity is more appropriately called a "binding energy" and it is not an appropriate measure of the stability of a complex with n H atoms in the vacancy. Indeed, a $V+n$H complex will only be stable if its energy is lower than the energy of a $V+(n-1)$H complex plus an isolated interstitial H; a quantity appropriately described by our definition of trapping energy in Eq. (6). We note that the trapping energy defined in Eq. (6) is equal to the negative of the "removal energy" defined in previous work.[25] The latter reflects how much energy is needed to remove one H atom from a complex initially con-

taining n H atoms, leaving $n-1$ H atoms behind and placing the H atom at an interstitial site.

In the case of Mg, we find that the trapping of multiple H atoms in single vacancies involves much smaller energies than in Al. A single vacancy in Mg can accommodate up to nine H atoms in a stable manner, as shown in Fig. 2. The reason for the difference with Al is that the increase in the trapping energy with the number of H atoms is less pronounced in Mg than in Al. A further difference to Al is that the OV sites are occupied in Mg for $V+n$H complexes already for $n>4$. This is due to the geometry of the hcp crystal structure in which the tetrahedral interstitial sites occur in pairs. Inside a vacancy, the four second-nearest-neighbor TV sites are occupied first, and then four OV sites and one TV site are occupied next. Hydrogen in molecular form is found to be unstable in single Mg vacancies.

E. Concentrations of hydrogen-vacancy complexes as a function of hydrogen chemical potential

So far we have discussed the trapping of H atoms in single vacancies. However, the overall likelihood of forming $V+n$H complexes depends on their formation energy and, therefore, on the hydrogen chemical potential μ_{H}. It also depends on the ratio of the hydrogen concentration to the vacancy concentration. For example, it is clear that it will be unlikely to find vacancies containing multiple H atoms if the hydrogen concentration in the metal is lower than the vacancy concentration. In this case it is entropically more favorable to distribute the hydrogen atoms over the vacancies with at most one H atom in each vacancy. We therefore expect that trapping of multiple H atoms will only occur if the H concentration is significantly higher than the vacancy concentration.

The formation energy of hydrogen-related defects according to Eq. (2) depends on the hydrogen chemical potential μ_{H}, which in turn depends on the type of hydrogen reservoir the solid is exposed to. For example, if the hydrogen is introduced in the metal through annealing in H_2 gas at a given temperature T and pressure p, the μ_{H} is a well-established function of p and T. High concentrations of hydrogen in the solid can also be obtained by annealing the metal under hot moist air,[26] via electrolytic charging,[27] or by exposure to a hydrogen plasma.[28] The values of μ_{H} in the latter experiments are much more difficult to assess and we will make no attempt to do so. Instead, we first simply plot our results as a function of μ_{H} to describe the general situation, detached from a specific hydrogen charging method. In addition, we look in more detail at one specific charging method, namely, the familiar situation of annealing in an H_2 gas at temperature T and pressure p, and plot our results as a function of pressure, for different fixed temperatures.

The chemical potential of the H_2 gas may be written as

$$\mu_{\mathrm{H}} = \frac{1}{2}\mu_{\mathrm{H}}^{0}(\mathrm{H}_2) + \mu_{\mathrm{H}}^{\mathrm{gas}}(T,p), \tag{8}$$

where μ_{H}^{0} is the hydrogen chemical potential in an H_2 molecule at $T=0$ K, i.e., the sum of the total energy and the zero-point vibration energy of the H_2 molecule. The temperature and pressure dependence of the chemical potential is described by the term $\mu_{\mathrm{H}}^{\mathrm{gas}}(T,p)$. For moderate temperatures and pressures (close to $T=300$ K and $p=1$ atm) this term is accurately described by an analytical expression arising from the ideal-gas approximation (see, e.g., Ref. 29). However, since we also wish to describe the chemical potential in the high-pressure regime $p \gg 1$ atm in which the ideal-gas approximation cannot be applied, we use tabulated experimental data.[20] In the following we neglect effects of vacancy clusters and extended defects such as dislocations and grain boundaries. Furthermore, we assume that the hydrogen concentration c_{H} and the vacancy concentration c_V in the host metal are small, i.e., $\ll 1$ (dilute limit).

The total vacancy concentration $c_{V_{\mathrm{tot}}}$ is then given by the sum of the concentration of isolated vacancies c_V and the concentration of vacancies participating in hydrogen-vacancy complexes $V+n$H, which we denote by $c_{V_{\mathrm{H}}}$. Note that while the formation energy of isolated vacancies does not depend on μ_{H}, the total vacancy concentration $c_{V_{\mathrm{tot}}}$ does, due to the hydrogen-vacancy interaction. Therefore, we have

$$c_{V_{\mathrm{tot}}} = c_V + c_{V_{\mathrm{H}}}, \tag{9}$$

where

$$c_V = \exp\left[-\frac{E^f(V)}{k_B T}\right] \tag{10}$$

and

$$c_{V_{\mathrm{H}}} = \sum_{n=1\cdots n^{\max}} S(n)\exp\left[-\frac{E^f(V+n\mathrm{H},\mu_{\mathrm{H}})}{k_B T}\right]. \tag{11}$$

Here, $n^{\max}$ is the maximum number of H atoms that can be trapped in the vacancies and ($n^{\max}=10$ for Al and $n^{\max}=9$ for Mg). $S(n)$ counts the number of possible configurations of the $V+n$H complex (i.e., the number of ways n indistinguishable H atoms can be distributed over the TV sites in a vacancy). We approximate $S(n)$ as $S(n)=\frac{n^{\max}!}{n!(n^{\max}-n)!}$; the only exception is for the $V+8\mathrm{H}+\mathrm{H}_2$ complex in Al ($n=10$), for which we set $S(n)=1$.

Similarly, the total hydrogen concentration $c_{\mathrm{H}_{\mathrm{tot}}}$ is given by the isolated hydrogen concentration c_{H} and the concentration of H in $V+n$H complexes $c_{\mathrm{H}_V}(n=1,\ldots,n^{\max})$,

$$c_{\mathrm{H}_{\mathrm{tot}}} = c_{\mathrm{H}} + c_{\mathrm{H}_V}, \tag{12}$$

where

$$c_{\mathrm{H}} = 2\,\exp\left[-\frac{E^f(T_d,\mu_{\mathrm{H}})}{k_B T}\right] \tag{13}$$

and

$$c_{\mathrm{H}_V} = \sum_{n=1\cdots n^{\max}} nS(n)\exp\left[-\frac{E^f(V+n\mathrm{H},\mu_{\mathrm{H}})}{k_B T}\right]. \tag{14}$$

The concentrations of hydrogen and vacancies as a function of the chemical potential μ_{H} in fcc Al and hcp Mg are shown in Figs. 4 and 5, respectively. We note that the hydrogen concentration at low hydrogen chemical potentials ($\mu_{\mathrm{H}}<0$) is much higher in hcp Mg than in fcc Al, whereas the

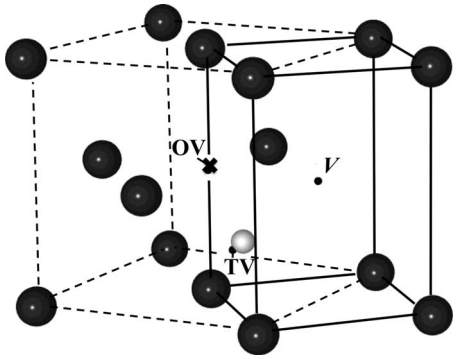

FIG. 3. Illustration of the lowest-energy structure for a single H atom trapped in a vacancy in fcc Al. The dark balls denote the positions of the atoms of the host lattice, whereas the white ball denotes the position of the H atom. Further shown are TV and OV trapping sites, and the center of the vacancy (labeled *V*). The dashed black lines show the conventional cubic unit cell of the fcc lattice, whereas the solid black lines outline the volume associated with the vacancy.

vacancy concentrations only differ by about an order of magnitude, consistent with the calculated formation energies listed in Table I.

An analysis of the dependence of the hydrogen and vacancy concentrations on the chemical potential μ_H shows that we can identify two regimes: for low values of μ_H, hydrogen exists mostly as isolated interstitial H atoms, i.e, $c_{H_{tot}} \approx c_H$, whereas the vacancy concentration is constant and independent of μ_H, i.e., $c_{V_{tot}} \approx c_V$. For high values of μ_H, a significant fraction of H atoms is trapped in vacancies. In this regime, $c_{H_{tot}}$ increases more rapidly with μ_H than c_H and $c_{V_{tot}}$ is not constant but also rapidly increases with μ_H. If we define a critical value μ_H^c for which the transition between these two regimes occurs, we find that μ_H^c is significantly lower in hcp Mg than in hcp Al; values for μ_H^c will be derived below. This result is attributed to the lower absolute formation energies of H-related defects in hcp Mg.

In Fig. 6 we plot the average number of H atoms that are trapped in vacancies in Al and Mg. We find that the concentration of $V+n$H complexes with $n>1$ becomes relevant only for values of $\mu_H > \mu_H^c$ for both Al and Mg. We note that differing from the previous work of Gunaydin *et al.*[9] who found a maximum of $n_H=6$, we find that $n_H=10$ for high values of μ_H in Al.

We observe that the trapping of multiple hydrogen atoms ($n_H>1$) occurs at the values of μ_H for which the vacancy concentration starts to rapidly increase. In other words, a rapid increase in the vacancy concentration will occur as soon as

$$E^f(V+\mathrm{H},\mu_H) < E^f(V). \tag{15}$$

Substituting Eq. (6) into Eq. (15) and using the expressions for formation energies, we obtain the following relation for μ_H^c above which H-enhanced vacancy formation occurs

$$\mu_H^c = E^f(T_d, \mu_H = 0) + E^{\mathrm{trap}}(1), \tag{16}$$

where $E^f(T_d, \mu_H=0)$ is the formation energy of hydrogen at the tetrahedral lattice site at $T=0$ K and $E^{\mathrm{trap}}(1)$ is the trapping energy for one H in a vacancy. Substituting the respective numbers for Mg and Al into Eq. (16) we obtain $\mu_H^c \approx 0.4$ eV for Al and $\mu_H^c \approx 0.1$ eV for Mg.

The trapping of multiple H atoms in turn is of fundamental importance for the occurrence of various mechanisms related to the H-vacancy interaction. As an example, we have already mentioned H-enhanced (superabundant) vacancy formation. The clustering of H-vacancy complexes, a process that is regarded as an initial step in the formation of hydro-

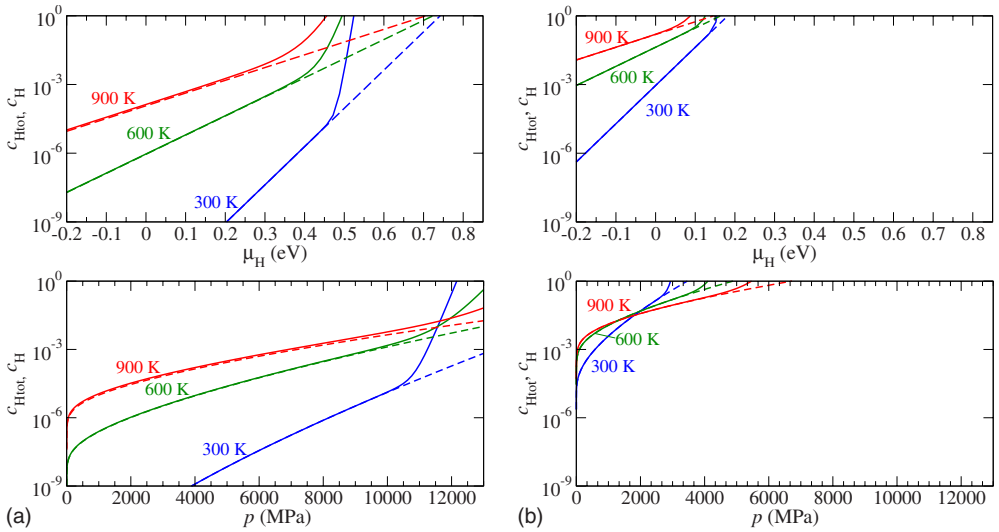

FIG. 4. (Color online) Hydrogen concentrations (in units per lattice site) in (a) Al and (b) Mg as a function of the hydrogen chemical potential (upper plots) and as a function of the pressure of H_2 gas (lower plots) for temperatures $T=300$, 600, and 900 K (blue, green, and red lines, respectively). The solid lines show the total hydrogen concentration $c_{H_{tot}}$, taking hydrogen-vacancy interactions into account [see Eq. (12)]. The dashed lines show the interstitial hydrogen concentration c_H, i.e., the hydrogen concentration in the absence of hydrogen-vacancy interactions. For convenience the horizontal axis showing the chemical potential in the upper plots has been shifted so that $\mu_H=0$ corresponds to half of the chemical potential of a H_2 molecule at $T=0$ K.

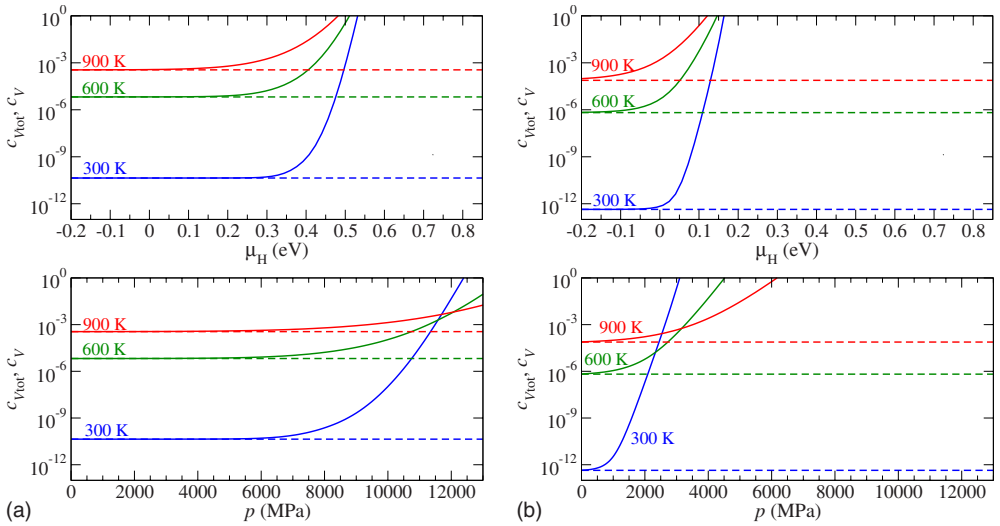

FIG. 5. (Color online) Vacancy concentration (in units per lattice site) in (a) Al and (b) Mg as a function of the hydrogen chemical potential (upper plots) and as a function of the pressure of H_2 gas (lower plots) for temperatures $T=300$, 600, and 900 K (blue, green, and red lines, respectively). The solid lines show the total vacancy concentration $c_{V_{tot}}$, taking hydrogen-vacancy interactions into account [see Eq. (9)]. The dashed lines show the vacancy concentration in the absence of hydrogen-vacancy interactions. For convenience the horizontal axis showing the chemical potential has been shifted so that $\mu_H=0$ corresponds to half of the chemical potential of a H_2 molecule at $T=0$ K.

gen bubbles[28] or of extended hydride platelets,[28] may well be driven by the trapping of multiple H atoms in vacancies.[8] Our results indicate that these phenomena will be observed at much more "moderate" hydrogen chemical-potential values in Mg than in Al. Expressed in terms of a hydrogen gas reservoir, these effects become relevant in Mg already at pressures of 1 GPa while in Al pressures as high as 10 GPa (or different hydrogen charging methods such as electrolytic charging or hydrogen plasmas) are required.

We note that the critical pressure for the occurrence of H-enhanced vacancy formation (and the trapping of multiple H atoms in vacancies) in Al is of the same order as the critical pressure required for AlH_3 hydride formation (8.9 GPa at room temperature[30]). This close correlation suggests that the processes of multiple trapping of H atoms and H-enhanced vacancy formation are probably involved in the process of hydride formation. A more detailed examination of this possibility requires going beyond the dilute limit which has been implicitly used in the present work and is beyond the scope of this study.

In Mg the critical pressure to induce hydride formation is much lower [about 0.1 MPa at $T=600$ K (Ref. 31)], i.e., below the critical pressure for H-enhanced vacancy formation derived here. Still, the processes that have been described here may be relevant under nonequilibrium conditions where hydride formation is suppressed or delayed.

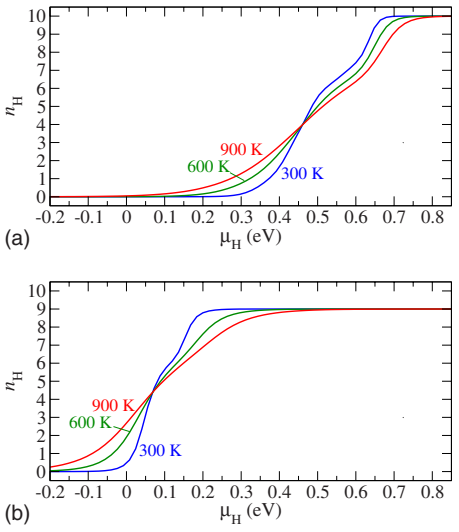

FIG. 6. (Color online) Average number of hydrogen atoms, n_H, trapped in the vacancies of (a) Al and (b) Mg. The plots show n_H as a function of the hydrogen chemical potential for temperatures $T=300$, 600, and 900 K (blue, green, and red lines, respectively). For convenience the horizontal axis showing the chemical potential has been shifted so that $\mu_H=0$ corresponds to half of the chemical potential of a H_2 molecule at $T=0$ K.

F. Effects of hydrogen-vacancy interactions on the hydrogen diffusivity

We have shown that the trapping of H atoms occurs at significantly lower hydrogen chemical potential in Mg than in Al. It is thus tempting to conclude that the H-vacancy interaction is, in general, more relevant in Mg than in Al. However a closer look at the fraction of hydrogen stored in vacancies $c_{H_V}/c_{H_{tot}}$ reveals an interesting feature of the H-vacancy interaction that has not yet been discussed so far. Figure 7 shows that in Al (but not in Mg), even at low hydrogen chemical potentials ($\mu_H \leq 0$) a significant fraction of the total hydrogen concentration (up to 15% at $T=900$ K) is located in the vacancies. Although this fraction is small in terms of the solubility of hydrogen in Al and plays no role in the enhanced vacancy formation mentioned above, it has distinct consequences for the diffusion of hydrogen impurities through the Al crystal.

An approximate expression to describe the impact of trapping on hydrogen diffusivity was derived by Oriani.[32] Re-

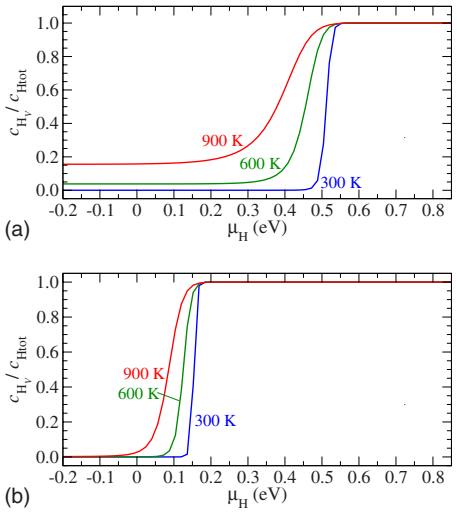

FIG. 7. (Color online) Fraction of hydrogen trapped in vacancies for (a) Al and (b) Mg. The plots show the ratio $c_{H_V}/c_{H_{tot}}$ as a function of the hydrogen chemical potential, for temperatures $T=300$, 600, and 900 K (blue, green, and red lines, respectively). c_{H_V} is the concentration of H trapped in vacancies [Eq. (14)] and $c_{H_{tot}}$ is the total hydrogen concentration [Eq. (12)]. For convenience the horizontal axis showing the chemical potential has been shifted so that $\mu_H=0$ corresponds to half of the chemical potential of a H_2 molecule at $T=0$ K.

writing the expressions from Ref. 32 in terms of hydrogen concentrations and trapping energies leads to

$$D^{\text{trap}} = \frac{D^{\text{lat}}}{1 + \frac{c_{H_V}}{c_{H_{tot}}} \exp\left(\frac{E^{\text{trap}}}{k_B T}\right)}. \tag{17}$$

Here D^{trap} is the diffusivity considering the presence of traps and D^{lat} is the bulk diffusivity in the absence of traps. Substituting the trapping energy and the hydrogen concentration ratios for Al we find, in agreement with the previous theoretical work of Ref. 9, that the diffusivity of H in Al is reduced by more than one order of magnitude at temperatures as high as 900 K, for any hydrogen chemical potential, i.e., at any hydrogen charging conditions. For Mg, in contrast, the vacancy trapping effect is negligible for low hydrogen chemical potentials since the fraction of hydrogen trapped in vacancies is less than 1% at these charging conditions.

The ratio $c_{H_V}/c_{H_{tot}}$ may in this context be understood as the probability for an individual H atom, from a reservoir of H atoms dissolved in the host metal, to be trapped in a vacancy. To understand the differences between Mg and Al in this respect we have derived a simple, approximate expression for the trapping probability at low hydrogen chemical potentials $\mu_H \ll \mu_H^c$. For the derivation we have introduced two approximations. First, we assume that the total concentration of hydrogen trapped in vacancies, c_{H_V}, is given by the concentration of hydrogen-vacancy complexes containing one hydrogen, c_{V+H}. This approximation is well justified since for $\mu_H \ll \mu_H^c$ we have $E^f[V+(n+1)H, \mu_H] > E^f(V+nH, \mu_H)$. Thus,

$$c_{H_V} \approx c_{V+H} = S(1) \exp\left(-\frac{E^f(V) + E^f(T_d, \mu_H) - |E^{\text{trap}}(1)|}{k_B T}\right). \tag{18}$$

Second, we exploit the fact that although up to 15% of the hydrogen is trapped in vacancies in Al for low μ_H at $T=900$ K, still at least 85% of the hydrogen is located at interstitial sites for $\mu_H \ll \mu_H^c$ (Fig. 7). In the case of Mg, the fraction of interstitial H at low μ_H is even larger. Using the fact that $c_H/c_{H_V} \gg 1$, we approximate $c_H/c_{H_V}+1 \approx c_H/c_{H_V}$. Using the two approximations we can rewrite the trapping probability as

$$\frac{c_{H_V}}{c_{H_{tot}}} = \left(1 + \frac{c_H}{c_{H_V}}\right)^{-1} \approx \frac{c_{H_V}}{c_H} \approx \frac{c_{V+H}}{c_H}. \tag{19}$$

Substituting Eqs. (13) and (18) into Eq. (19) yields

$$\frac{c_{H_V}}{c_{H_{tot}}} \approx \frac{S(1)}{2} \exp\left[-\frac{E^f(V)}{k_B T}\right] \exp\left[\frac{|E^{\text{trap}}(1)|}{k_B T}\right]. \tag{20}$$

According to Eq. (20), at low μ_H the trapping probability of an individual H atom is independent of the formation energy of interstitial hydrogen in the metal and thus independent of the hydrogen chemical potential. Equation (20) further reveals that the trapping probability is proportional to the vacancy concentration and to a Boltzmann factor involving the absolute value of the trapping energy. The fact that the trapping probability is significantly higher in Al than in Mg can thus be explained by the higher (absolute) value of the trapping energy and the (slightly) lower formation energy of vacancies in Al.

IV. SUMMARY

We have shown that single vacancies in the host metal can host up to nine H atoms in Mg and ten in Al, not 12 as recently reported in the case of Al.[8] This difference can be attributed to a more appropriate definition of the trapping energy, at variance with the previous work.[8] In principle multiple H atoms can therefore be trapped in a vacancy; however, in practice incorporating more than one hydrogen atom into a vacancy requires extremely high hydrogen concentrations, which in turn can only be achieved at very high values of the hydrogen chemical potential.

Indeed, we find that the character of the hydrogen-vacancy interaction and the likelihood of trapping multiple H atoms strongly depends on the amount of hydrogen dissolved in the metal (which is dictated by the hydrogen chemical potential) and on the ratio of the concentration of hydrogen to the concentration of naturally occurring vacancies in the host metal.

Our analysis reveals fundamental differences for the characteristics of the H-vacancy interaction between Al and Mg. In Al, trapping of multiple H atoms in vacancies and the various processes related to it (such as H-enhanced vacancy

formation and possible vacancy clustering) occur only for relatively high hydrogen chemical potentials ($\mu_H > \mu_H^c \approx 0.4$ eV), which would require H_2 gas at a pressure of 10 GPa or a hydrogen plasma. In Mg more moderate conditions are sufficient, corresponding to a hydrogen chemical potential $\mu_H > \mu_H^c \approx 0.1$ eV, which corresponds to an H_2 gas pressure of 1 GPa. The difference is attributed to the fact that more hydrogen is dissolved in Mg than in Al at a given chemical potential and thus the hydrogen concentration in Mg exceeds the vacancy concentration by several orders of magnitude.

Nonetheless, in Al a small fraction (up to 15%) of H atoms is trapped in single-H-vacancy complexes already at low hydrogen chemical potentials. This trapping effect slows down the diffusion of H atoms through the Al lattice by more than an order of magnitude. This effect is not found for Mg, mainly because in Mg the (absolute) value of the trapping energy is smaller than in Al.

ACKNOWLEDGMENTS

We thank J. Neugebauer for fruitful discussions. This work was supported by the U. S. Department of Energy (Grant No. DE-FG02-07ER46434). It made use of the CNSI Computing Facility under NSF Grant No. CHE-0321368 and the NSF-funded TeraGrid resources under Grant No. DMR070072N. L.I. thanks the UCSB-MPG Program for International Exchange in Materials Science and the NSF-IMI Program (Grant No. DMR04-09848) for financial support.

[1] J. Graetz, Chem. Soc. Rev. **38**, 73 (2009).
[2] K. Dorenburg, M. Gladisch, D. Herlach, W. Mansel, H. Metz, H. Orth, G. zu Pulitz, A. Seeger, W. Wahl, and M. Wigand, Z. Phys. B **31**, 165 (1978).
[3] W. J. Kossler, A. T. Fiory, W. F. Lankford, K. G. Lynn, R. P. Minnich, and C. E. Stronach, Hyperfine Interact. **6**, 295 (1979).
[4] J. P. Bugeat, A. C. Chami, and E. Ligeon, Phys. Lett. A **58**, 127 (1976).
[5] D. S. Larsen and J. K. Nørskov, J. Phys. F: Met. Phys. **9**, 1975 (1979).
[6] G. A. Young and J. R. Scully, Acta Mater. **46**, 6337 (1998).
[7] C. Wolverton, A. Ozolins, and M. Asta, Phys. Rev. B **69**, 144109 (2004).
[8] G. Lu and E. Kaxiras, Phys. Rev. Lett. **94**, 155501 (2005).
[9] H. Gunaydin, S. V. Barabash, K. N. Houk, and V. Ozolins, Phys. Rev. Lett. **101**, 075901 (2008).
[10] A. C. Chami, J. P. Bugeat, and E. Ligeon, Radiat. Eff. **37**, 73 (1978).
[11] M. Yamada, M. Hida, and T. Senuma, Mater. Trans. **49**, 2006 (2008).
[12] C. G. Van de Walle and J. Neugebauer, J. Appl. Phys. **95**, 3851 (2004).
[13] J. Perdew, J. Chevary, S. Vosko, K. Jackson, M. Pederson, D. Singh, and C. Fiolhais, Phys. Rev. B **46**, 6671 (1992).
[14] P. Blöchl, Phys. Rev. B **50**, 17953 (1994).
[15] G. Kresse and J. Furthmüller, Phys. Rev. B **54**, 11169 (1996).
[16] R. A. H. Edwards and W. Eichenauer, Scr. Metall. **14**, 971 (1980).
[17] W. Eichenauer, K. Hattenbach, and A. Pebler, Z. Metallkd. **52**, 682 (1961).
[18] W. Eichenauer, Z. Metallkd. **59**, 613 (1968).
[19] H. Ichimura, H. Katsuta, Y. Sasajima, and M. Imabayashi, J. Phys. Chem. Solids **49**, 1259 (1988).
[20] H. Sugimoto and Y. Fukai, Acta Metall. Mater. **40**, 2327 (1992).
[21] T. Vegge, Phys. Rev. B **70**, 035412 (2004).
[22] C. Nishimura, M. Komaki, and M. Amano, J. Alloys Compd. **293-295**, 329 (1999).
[23] M. J. Fluss, L. C. Smedskjaer, M. K. Chason, D. G. Legnini, and R. W. Siegel, Phys. Rev. B **17**, 3444 (1978).
[24] C. Huang and E. A. Carter, Phys. Chem. Chem. Phys. **10**, 7109 (2008).
[25] C. G. Van de Walle, Phys. Rev. B **56**, R10020 (1997).
[26] M. Bobby Kannan and V. S. Raja, J. Mater. Sci. **41**, 5495 (2006).
[27] H. Birnbaum, C. Buckley, F. Zeides, E. Sirois, P. Rozenak, S. Spooner, and J. Lin, J. Alloys Compd. **253-254**, 260 (1997).
[28] C. Buckley, H. Birnbaum, J. Lin, S. Spooner, D. Bellmann, P. Staron, T. Udovic, and E. Hollar, J. Appl. Crystallogr. **34**, 119 (2001).
[29] H. Wipf, Phys. Scr., T **T94**, 43 (2001).
[30] H. Saitoh, A. Machida, Y. Katayama, and K. Aoki, Appl. Phys. Lett. **93**, 151918 (2008).
[31] L. Schlapbach and A. Züttel, Nature (London) **414**, 353 (2001).
[32] R. A. Oriani, Acta Metall. **18**, 147 (1970).